

Deuteration effect on tricritical phase transition of triglycine selenate: Calorimetric and dielectric measurements analyzed in the framework of Landau theory

Cite as: J. Appl. Phys. **107**, 124110 (2010); <https://doi.org/10.1063/1.3452365>

Submitted: 24 February 2010 . Accepted: 15 May 2010 . Published Online: 24 June 2010

F. J. Romero, M. C. Gallardo, J. M. Martín-Olalla, and J. del Cerro



View Online



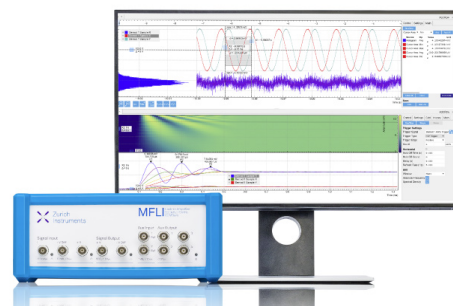
Export Citation

Challenge us.

What are your needs for periodic signal detection?



Zurich
Instruments



Deuteration effect on tricritical phase transition of triglycine selenate: Calorimetric and dielectric measurements analyzed in the framework of Landau theory

F. J. Romero,^{a)} M. C. Gallardo, J. M. Martín-Olalla, and J. del Cerro

Departamento de Física de la Materia Condensada, Instituto Mixto de Ciencia de Materiales ICMSE-CSIC, Universidad de Sevilla, Apartado 1065, 41080 Sevilla, Spain

(Received 24 February 2010; accepted 15 May 2010; published online 24 June 2010)

The ferroelectric phase transition of three single crystals of $(\text{TGSe})_{1-x}(\text{DTGSe})_x$ has been described by using specific heat, latent heat, and dielectric permittivity measurements. Pure, half-deuterated, and highly-deuterated TGSe single crystals were analyzed. Transition temperature and latent heat increase with increasing deuteration. Irrespective of the degree of deuteration, a 2-4-6 Landau model is suitable to describe the phase transition. The fourth-rank prefactor in Landau potential is found to be very sensitive to deuteration while the second-rank and the sixth-rank prefactors smoothly change with composition. The pyroelectric figure of merit for these materials has also been derived from the theoretical model. © 2010 American Institute of Physics. [doi:10.1063/1.3452365]

I. INTRODUCTION

Compositional changes alter most ferroelectric phase transitions. Their influence is greatly significant if the phase transition happens to be close enough to a tricritical point (TCP), where the first or second order nature of the phase transition can be modified by such a change. Specifically, the hydrogen-bonded ferroelectrics are known to be very sensitive to deuteration.¹⁻⁷

As a paradigm of this behavior, triglycine selenate $(\text{NH}_2\text{CH}_2\text{COOH})_3\text{H}_2\text{SeO}_4$, hereafter TGSe, is a well known uniaxial, ferroelectric material belonging to the triglycine sulfate (TGS) family, which exhibits an order-disorder phase transition^{8,9} (from high temperature space group $P2_1/m$ to low temperature space group $P2_1$) at $T=295$ K. These crystals have applications as infrared detectors and vidicons. For instance, TGS has attracted great interest for the development of infrared sensors^{10,11} and flat-panel displays^{12,13} due to its large pyroelectric coefficient¹⁴ and large pyroelectric figure of merit.¹⁵ It has been suggested¹⁶ that TGSe could have better pyroelectric properties at low temperatures than TGS and that deuteration on TGSe could improve such properties. Nevertheless, the influence of deuteration on specific heat was not taken into account and the pyroelectric performance of a material is best described through its thermal and dielectric properties. Thus, the measurement and characterization of these properties could be valuable for determining the potential application of a material.

Recently, the phase transition of a high-purity single crystal of TGSe at $T=295$ K was analyzed by means of calorimetric measurements.¹⁷ No latent heat was observed, showing, within the experimental resolution, that the phase transition was continuous. The specific heat of the ferroelectric phase was found to follow a classical tricritical Landau potential, whose coefficients were determined.

Earlier studies^{5,18,19} on the dielectric permittivity of deuterated samples of triglycine selenate, $(\text{TGSe})_{1-x}(\text{DTGSe})_x$, have shown that thermal hysteresis increases with increasing deuteration, suggesting that the phase transition evolves to a first-order phase transition when the sample is deuterated.

Detailed studies of the thermal properties are advantageous in determining the thermodynamic parameters characterizing a phase transition. The presence of latent heat confirms the discontinuous character of a phase transition and the specific heat integrates the contributions to the free energy. Furthermore, the analysis of thermal properties in the framework of Landau theory is appropriate to describe phase transitions whose nature is modified by different parameters such as pressure or compositional changes because their influence can be characterized by changes in the coefficients of the Landau potential.

The specific heat and latent heat of a partially deuterated sample ($x=0.62$) were reported.^{20,21} The specific heat of the sample was studied in the framework of a Landau potential whose coefficients were computed, despite the few experimental data in the analysis. Yet, the study did not focus on the influence of deuteration on the calorimetric properties; rather, it analyzed the influence of γ -irradiation.

Recently, dielectric and calorimetric measurements on a sample of $(\text{TGSe})_{1-x}(\text{DTGSe})_x$ with $x=0.9$ were also reported²² including latent heat. The whole set of experimental data were successfully described through a 2-4-6 classical Landau potential, whose coefficients were also determined. The influence of a longitudinal electric field in calorimetric and dielectric properties of $(\text{TGSe})_{1-x}(\text{DTGSe})_x$ with $x=0.9$ was also reported.²³ On cooling experiments, data and Landau theory expectations were found to be in full agreement.

The measurement of different properties such as specific heat, latent heat, and dielectric permittivity should be of the greatest convenience. Since data were reported for an almost fully deuterated sample as well as for a nondeuterated sample, it is mandatory to measure thermophysical properties on half-deuterated samples with the idea of providing a

^{a)}Electronic mail: fjomero@us.es.

comprehensive analysis of the influence of deuteration. This analysis should also include a common model able to explain the behavior of these properties regardless the degree of deuteration in the sample. That is the goal of this paper.

Our group has developed an original technique^{24,25} based on conduction calorimetry and referred to as squared modulated differential thermal analysis (SMDTA), which provides absolute values of the specific heat and allows latent heats to be determined separately, even in the case of phase transitions close to a TCP. For example, the almost tricritical phase transition in $\text{KMn}_{1-x}\text{Ca}_x\text{F}_3$ was studied. It was shown that phase transition shifts from first to second order as Ca doping increases.^{24,26} The solid solution was studied in the framework of the Landau theory and the coefficients of the potential were obtained for different dopant concentrations.²⁷

Influence of deuteration on $(\text{TGSe})_{1-x}(\text{DTGSe})_x$ in excess specific heat, latent heat, and dielectric permittivity has been studied using the above method. Latent heat and excess specific heat have been measured on the same device and under the same experimental conditions. The experimental data have been analyzed in the framework of the Landau theory, whose coefficients have been also determined.

II. EXPERIMENTAL

Three single crystals of $(\text{TGSe})_{1-x}(\text{DTGSe})_x$, with $x=0$, $x=0.5$, and $x=0.9$, were prepared at the Institute of Physics, Adam Mickiewicz University, Poznan, Poland. The crystals were grown from an aqueous solution by slow evaporation of water at constant temperature above the Curie point. The ferroelectric axis, **b**-axis, was determined by the cleavage plane (010). The fragility of the sample increased with deuteration, so that the most deuterated sample showed an internal break which may influence the kinetics of the transition. The samples were 0.2566 g, 0.3436 g, and 0.3494 g in mass, 54.44 mm², 67.05 mm², and 70.52 mm² in cross section and 2.72 mm, 2.89 mm, and 2.55 mm in width, respectively. Gold electrodes were evaporated on the main faces, perpendicular to the ferroelectric axis.

The measurements of the specific heat were carried out in a high resolution conduction calorimeter, which was previously described in detail.²⁸ The absolute value for specific heat is obtained by integrating the electromotive force given by two heat fluxmeters when the temperature of the sample changes as a consequence of the superposition of a long-periodic series of square thermal pulses to a heating or cooling ramp.^{24,29}

In a second run, the equipment worked as a high sensitive (better than 100 nW) differential thermal analysis (DTA) device. The high thermal stability of the device allows a temperature change rate similar to that used for measuring heat capacity. The latent heat is obtained by comparing the DTA trace and the specific heat data, following a method also described previously.²⁶ The sensitivity of this method is estimated to be better than 5 mJ, even when the specific heat shows a strong anomaly at the transition. Moreover, these measurements can be taken under the influence of external fields, such as an electric field or an uniaxial stress.

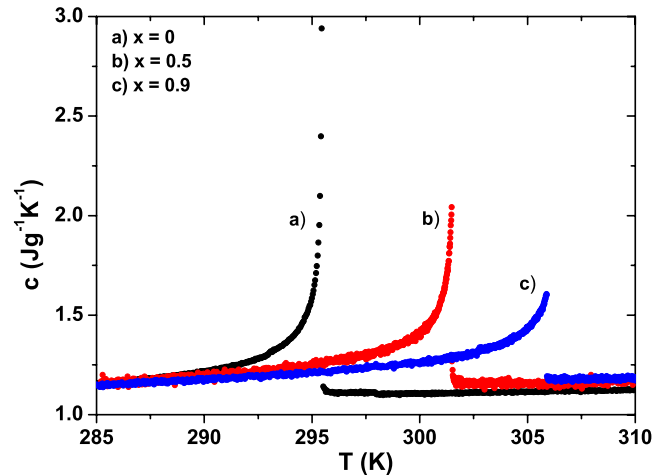


FIG. 1. (Color online) Specific heat of $(\text{TGSe})_{1-x}(\text{DTGSe})_x$ single crystals with $x=0, 0.5$, and 0.9 as obtained in the experiments on cooling.

The dielectric permittivity was measured by a capacitance bridge ESI-SP 5400 at a working frequency of 1 kHz in a different cell.

III. RESULTS

A. Thermal properties

The specific heat c of $(\text{TGSe})_{1-x}(\text{DTGSe})_x$ single crystals with $x=0, 0.5, 0.9$ was recorded in cooling and heating runs at a scanning temperature rate of 0.03 K h^{-1} . In Fig. 1, cooling data are shown in a temperature interval of 25 K around the transition temperature. The specific heats show a linear temperature dependence in the paraelectric phase. Nondeuterated TGSe shows a sharp λ -like anomaly around the transition temperature. The specific heat decreases by a 80% in 0.5 K from the peak.¹⁷

As deuteration increases, the temperature of maximum specific heat increases and the maximum of the specific heat decreases. The decrease in the maximum of the specific heat is showing that the transition moves away from the TCP.

The relevant magnitude to make a comparison with a theoretical model for a phase transition is the excess specific heat Δc , obtained after subtracting an appropriate baseline. This regular background contribution was taken as a linear extrapolation of the specific heat of the paraelectric phase well above the phase transition. The excess specific heat data are shown in Fig. 2 in a narrow temperature interval.

Data for pure TGSe show no hysteresis. For the deuterated samples, the specific heat on heating runs behaves the same as data in cooling experiments, but the transition takes place at a higher temperature showing thermal hysteresis. It is an indication that transition becomes first-order when the sample becomes deuterated. It should be also mentioned that the transition widens out with increasing deuteration; the excess specific heat decreases by 80% from peak value in 0.5, 1.5, and 3 K as deuteration increases.

In a second experiment, DTA traces were obtained changing the temperature at a constant rate of 0.1 K h^{-1} . Figure 3 shows DTA traces for the samples with $x=0.5$ and 0.9 . The phase transition is carried out through partial transformations, resulting in isolated peaks in the trace. These

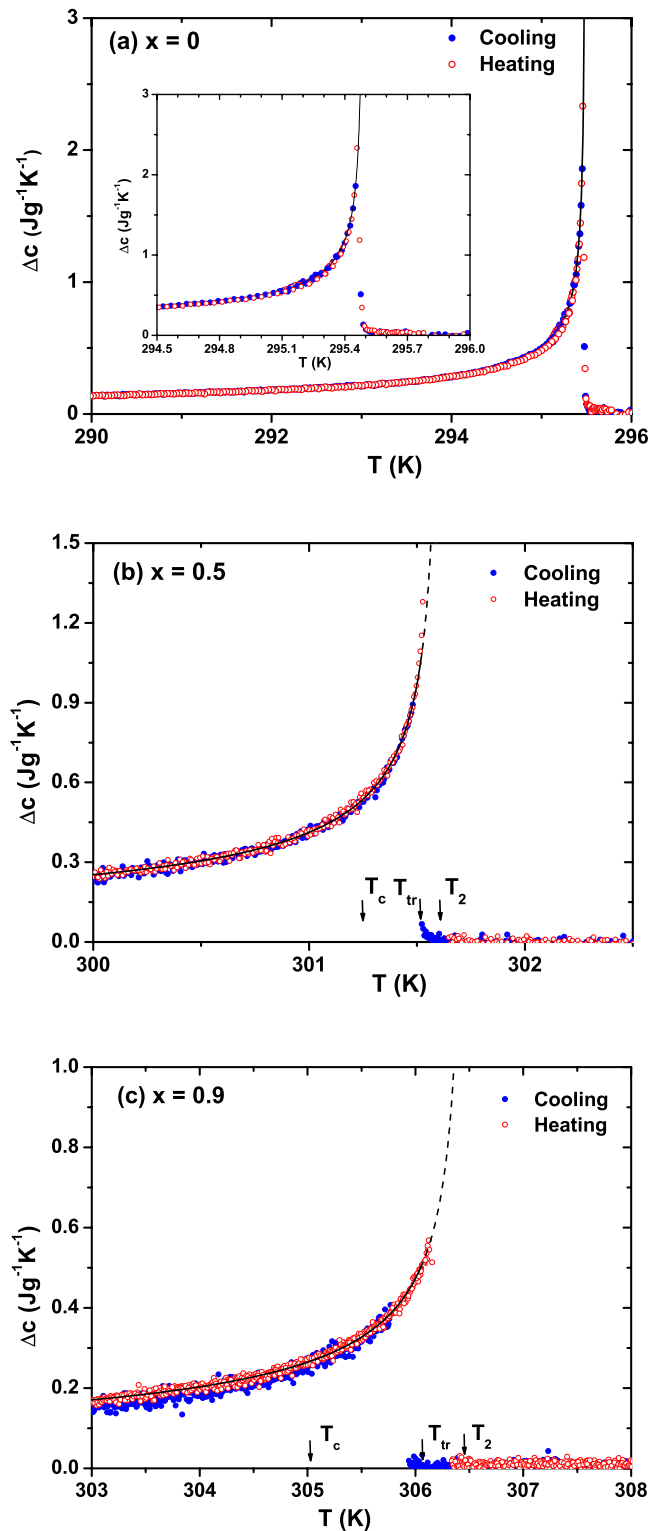


FIG. 2. (Color online) Excess specific heat vs temperature for $(\text{TGSe})_{1-x}(\text{DTGSe})_x$ with (a) $x=0$, (b) $x=0.5$, and (c) $x=0.9$ on cooling runs (solid circles) and heating runs (open circles). The predictions computed from Landau theory are also shown: solid lines for stable values and dashed lines for metastable values. Calculated characteristic temperatures are shown by arrows.

partial transformations are related to the kinetics of the phase transition. The phase transition is observed to take place more abruptly in cooling runs.

Latent heats were determined by integrating the heat flux peak in the DTA trace after having subtracted the appropriate

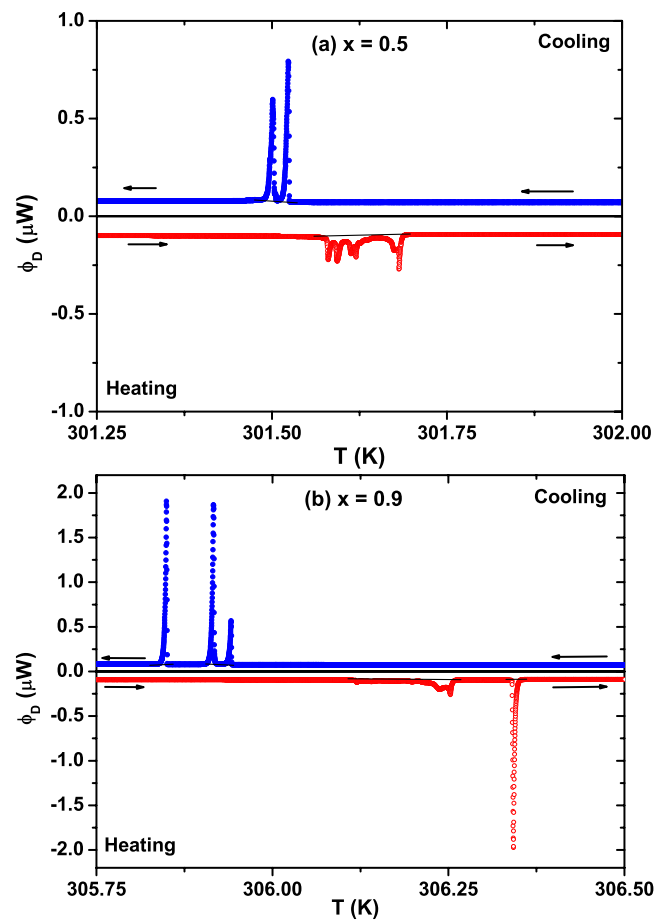


FIG. 3. (Color online) DTA trace for $x=0.5$ and 0.9 on heating and cooling runs.

background contribution due to the specific heat of the sample using a method described elsewhere.^{25,26} The latent heat data are listed in Table I. It should be stressed that the latent heat measured during cooling runs is larger than during heating runs. That is due to the fact that the excess specific heat in heating runs is larger than in cooling runs and contributes more to the enthalpy. Accordingly, L must be smaller in heating runs than in cooling runs in order to maintain the enthalpy balance.

To check this statement, the enthalpy balance for deuterated samples was computed. The integration of the heat flux provides the change of enthalpy, including both the contribution due to latent heat and the contribution due to specific heat. Figure 4 shows the enthalpy difference between a state in the paraelectric phase, which is taken as a reference, and a state in the ferroelectric phase on cooling and heating runs for $x=0.5$. The corresponding figure for $x=0.9$ was reported previously.²⁵ Despite the kinetical differences of both trans-

TABLE I. Absolute values of the latent heat for $(\text{TGSe})_{1-x}(\text{DTGSe})_x$ on cooling runs L_c and on heating runs L_h .

x	L_h (J g^{-1})	L_c (J g^{-1})
0.5	0.50(2)	0.66(2)
0.9	1.08(2)	1.32(2)

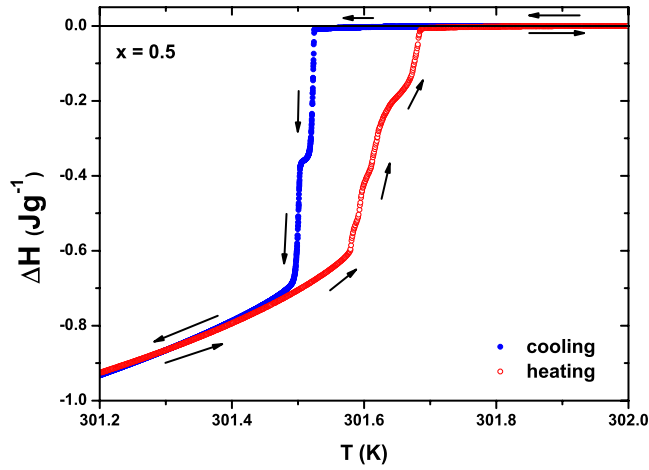


FIG. 4. (Color online) Enthalpy balance for $x=0.5$ near the transition temperature.

formations and the different magnitude of the steps due to latent heat contributions, enthalpy balance is fulfilled.

B. Dielectric permittivity

The dielectric permittivity of $(\text{TGSe})_{1-x}(\text{DTGSe})_x$ for $x=0, 0.5$, and 0.9 was recorded at a scanning rate of 0.5 K h^{-1} in a different cell to that used for calorimetric measurements. Permittivity was recorded several times on different scanning rates, on both cooling runs and heating runs, for each of the samples.

Dielectric permittivity data in deuterated samples are shown in Fig. 5. They exhibit repeatability in the paraelectric phase. Transition temperature and hysteresis increases with deuteration, while, on the contrary, peak value decreases. In the paraelectric phase, the Curie–Weiss law $\varepsilon = C_{\text{CW}}/(T - T_c)$ is fulfilled with a Curie–Weiss constant equal to 3700 K and 4700 K for $x=0.5$ and $x=0.9$, respectively. The Curie–Weiss behavior is also shown in Fig. 5. The Curie–Weiss constant C_{CW} increases with increasing deuteration in agreement with earlier results.^{2,30}

On the contrary, data of the nondeuterated sample ($x=0$) exhibits lack of repeatability in the paraelectric phase

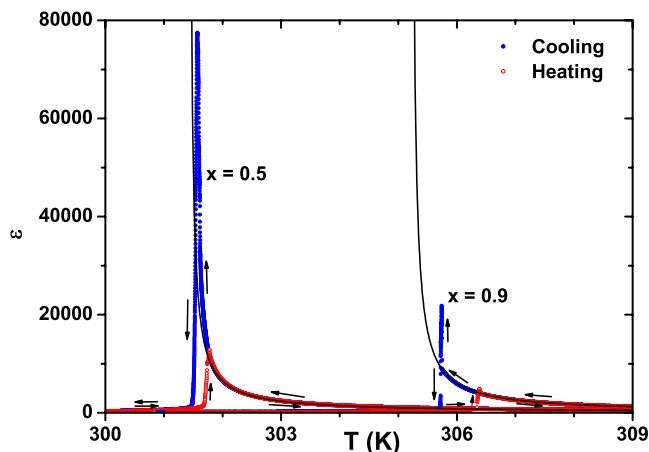


FIG. 5. (Color online) Dielectric permittivity data on heating and cooling runs for $(\text{TGSe})_{1-x}(\text{DTGSe})_x$ with $x=0.5$ and 0.9 . Solid lines are the fitted Curie–Weiss behavior.

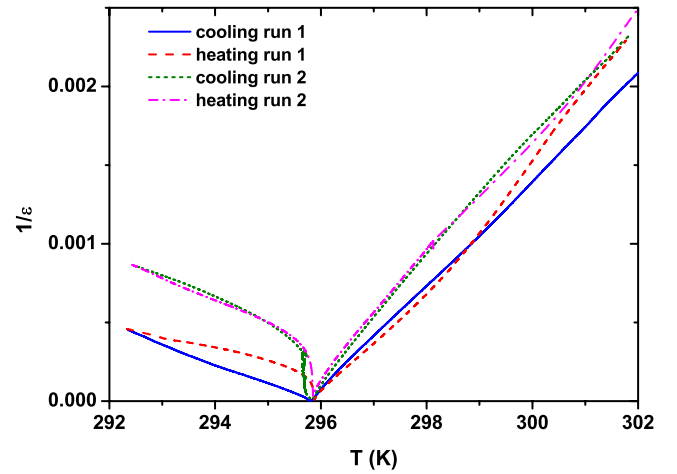


FIG. 6. (Color online) Inverse of the dielectric permittivity for nondeuterated TGSe ($x=0$) on heating and cooling runs.

when the sample is cooled and heated successively (see Fig. 6). This fact could be related to the relaxation process due to close vicinity to the TCP, where dielectric permittivity is expected to tend to infinity at T_c . In experiments, dielectric permittivity does not diverge at T_c due to, for instance, surface layer effect, inhomogeneities and local electric fields which could be present even in the paraelectric phase.³¹ Hence, it is not possible to get the Curie–Weiss constant for this sample.

IV. DISCUSSION

The Landau theory provides a theoretical framework for describing phase transitions whose nature could be modified by different parameters such as pressure or compositional changes. For near-tricritical phase transitions, the excess free energy ΔG is expanded in even power series of the order parameter Q up to the sixth order

$$\Delta G = \frac{1}{2}A(T - T_c)Q^2 + \frac{1}{4}BQ^4 + \frac{1}{6}CQ^6, \quad (1)$$

where A , B , and C are assumed to be independent of temperature. The coefficients A and C take positive values and the character of the transition depends on the sign of the fourth-rank prefactor B . The potential describes first-order phase transitions if $B < 0$ and second-order phase transitions for $B > 0$. The TCP is realized at $B=0$.

Although Eq. (1) successfully describes first-order, tricritical, and second-order phase transitions, the adjustable parameters A , B , C , and T_c are determined from experimental data in different ways in each case.

For the first-order phase transition, which is the case of the deuterated samples, the fitting procedure will be similar to that described previously in the analysis of $\text{KMn}_{1-x}\text{Ca}_x\text{F}_3$,^{32,33} where the specific heat anomaly and measured latent heat were used to constrain the Landau potential. First, the behavior of the specific heat as a function of temperature derived from Eq. (1) gives the following linear dependence:

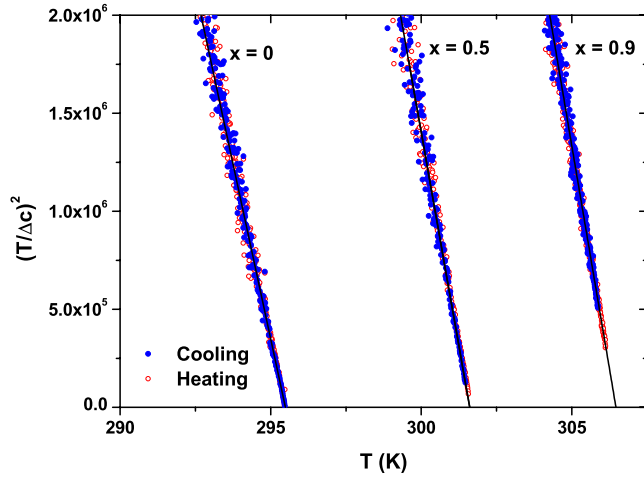


FIG. 7. (Color online) $(T/\Delta c)^2$ of $(\text{TGSe})_{1-x}(\text{DTGS})_x$ single crystals with $x=0, 0.5$, and 0.9 .

$$\left(\frac{T}{\Delta c}\right)^2 = \frac{4B^2 + 16AC(T - T_c)}{A^4}. \quad (2)$$

In a first-order phase transition, it is more convenient to introduce three different temperatures: T_c , T_{tr} , and T_2 . T_{tr} is the phase equilibrium temperature, i.e., when $\Delta G_{\text{ferro}} = \Delta G_{\text{para}}$. T_2 is the highest temperature at which the ferroelectric phase may exist, in contrast to T_c which is the lowest temperature at which the paraelectric phase may exist. These temperatures are related by

$$T_2 - T_c = 4(T_2 - T_{tr}) = \frac{B^2}{4AC}. \quad (3)$$

Thus, the temperature extent of the two phase region (and hence the maximum thermal hysteresis) is given by $d = T_2 - T_c$. However, experimental thermal hystereses are usually lower than this theoretical value. Incidentally, these three temperatures match each other (and d equals to zero) for a tricritical phase transition, where $B=0$.

For a first-order transition, the magnitude of the order parameter discontinuity or, alternatively, the latent heat, plays an important role in characterizing the transition. The latent heat is theoretically defined from the step which the entropy excess ΔS would show if the transition took place at T_{tr} (in equilibrium of phases) and it is related to the coefficients by

$$L = \frac{3AB}{8C} T_{tr}. \quad (4)$$

When the latent heat is measured, two different values are obtained, one on heating L_h and another on cooling L_c . The

theoretical latent heat L should lie in this range. The measured mean value will be taken in the fitting procedure.

Equation (2) can be then rewritten including T_2 as

$$\left(\frac{T}{\Delta c}\right)^2 = m(T_2 - T), \quad (5)$$

where

$$m = \frac{16C}{A^3}. \quad (6)$$

Figure 7 shows the behavior of $(T/\Delta c)^2$ versus T for the three samples along with the fitted straight lines which set the values for T_2 and m (see Table II). Experimental data and fitted expressions agree, showing that the behavior of these systems follows a 2-4-6 Landau classical potential.

After the applicability of the Landau model has been checked, coefficients A , B , and C must be found. For first-order phase transitions, the gradient of $(T/\Delta c)^2$ versus T , m , can be rewritten³² in terms of the latent heat L , the extent of the two phase region on the phase diagram d and the characteristic temperature T_2

$$m = \frac{9d(T_2 - d/4)^2}{L^2}. \quad (7)$$

Parameter d is obtained from Eq. (7) after introducing the experimental value for L and the fitted values for T_2 and m . Temperatures T_c and T_{tr} are then computed from Eq. (3). Table II lists the values for d , T_c , and T_{tr} .

Finally, the coefficients in Eq. (1) can be obtained. Equations (3) and (4) provide B and C in terms of A

$$B = \frac{3dT_{tr}A^2}{2L}, \quad (8)$$

$$C = \frac{9dT_{tr}^2A^3}{16L^2}. \quad (9)$$

so that it is necessary to obtain previously the prefactor A .

In ferroelectric phase transitions, the coefficient A is usually obtained from the dielectric constant measurements. If the polarization P is taken as the order parameter in Eq. (1), the Landau potential is written as

$$\Delta G = \frac{1}{2}\alpha(T - T_c)P^2 + \frac{1}{4}\beta P^4 + \frac{1}{6}\gamma P^6, \quad (10)$$

where the greek letters will stress the choice of P . The coefficient α could be obtained from the dielectric constant measurements, since it is related to the Curie-Weiss constant C_{CW} by $\alpha = 1/(\epsilon_0 C_{CW})$. For the deuterated samples, α could

TABLE II. Results of the linear fitting $(T/\Delta c)^2 = m(T_2 - T)$ in the ferroelectric phase for $(\text{TGSe})_{1-x}(\text{DTGS})_x$ with $x=0, 0.5$ and $x=0.9$. T_{tr} , T_c , and d obtained from Eqs. (3) and (7) are also included. The uncertainties of m and T_2 have been obtained from the least-squares linear fitting.

x	m ($\text{J}^{-2} \text{g}^2 \text{K}^3$)	T_2 (K)	T_{tr} (K)	T_c (K)	d (K)
0	$713(12) \times 10^3$	295.50(1)	...	295.47(2)	
0.5	$871(15) \times 10^3$	301.61(1)	301.52(1)	301.25(3)	0.36(2)
0.9	$910(18) \times 10^3$	306.46(1)	306.07(2)	304.91(5)	1.55(5)

TABLE III. Computed values of the coefficients A , B , C , and T_c in the Landau potential [see Eq. (1)] for $(\text{TGSe})_{1-x}(\text{DTGSe})_x$ with $x=0$, $x=0.5$, and $x=0.9$.

x	A ($\text{J g}^{-1} \text{K}^{-1}$)	B (J g^{-1})	C (J g^{-1})	T_c (K)
0	0.0816(7)	0	24.1(2)	295.47(2)
0.5	0.0770(6)	-1.66(6)	24.9(2)	301.25(3)
0.9	0.0786(7)	-3.68(5)	27.7(2)	304.91(5)

be obtained from the measured C_{CW} . Nevertheless, α cannot be obtained for the nondeuterated sample ($x=0$) due to the lack of repeatability in dielectric data (see Sec. III B).

As an alternative the order parameter in Eq. (1) will be taken as $Q=P/P_0$, where P_0 is the polarization at 0 K. In this way, Q is normalized to unity at that temperature. This choice is also useful when different materials are to be compared (different values of P_0 are expected for each material) and also when it is difficult the measurement of the order parameter susceptibility, as occurs with ferroelastic materials. In any case, the coefficients α , β , and γ are related to A , B , and C by

$$\rho A = \alpha P_0^2, \quad \rho B = \beta P_0^4, \quad \rho C = \gamma P_0^6, \quad (11)$$

where ρ is the density and $P_0^2 = \rho \varepsilon_0 A C_{\text{CW}}$.

The coefficient A will be computed directly from the condition of normalization of the order parameter ($Q=1$ at $T=0$). The equation of state, obtained from the vanishing of the first derivative of Eq. (1) on Q , is given by

$$A(T - T_c)Q + BQ^3 + CQ^5 = 0. \quad (12)$$

Computing this equation at $T=0$ reduces it to

$$B + C - AT_c = 0. \quad (13)$$

Hence, the set of Eqs. (3), (4), and (13) suffices for determining A , B , and C . The coefficient A is given by

$$A = \frac{-4L}{3T_{tr}} \left\{ 1 + \sqrt{\frac{T_2}{d}} \right\}. \quad (14)$$

B and C are then computed from Eqs. (8) and (9). This method was previously considered for analyzing the KMnF_3 ferroelastic system.^{32,33}

In the case of nondeuterated TGSe ($x=0$), no evidence of latent heat was found¹⁷ and the sharpness of the specific heat anomaly suggested that the temperature of maximum specific heat T_m could be taken as T_c . The difference $T_2 - T_c$, evaluated to be 0.03 K, was assumed to be within the experimental temperature resolution, so that, $T_c \approx T_2$ and, following Eq. (3), $B \approx 0$. From Eq. (13), $AT_c = C$ and the gradient of $(T/\Delta c)^2$ versus T , m , sets the value for A and, consequently, C .

Table III lists the obtained values for A , B , and C . Coefficients A and C are rather insensitive to change in x . On the contrary, B and T_c are sensitive to it. Coefficient B becomes more negative as deuteration increases and T_c also increases with deuteration. The strong influence of x in B

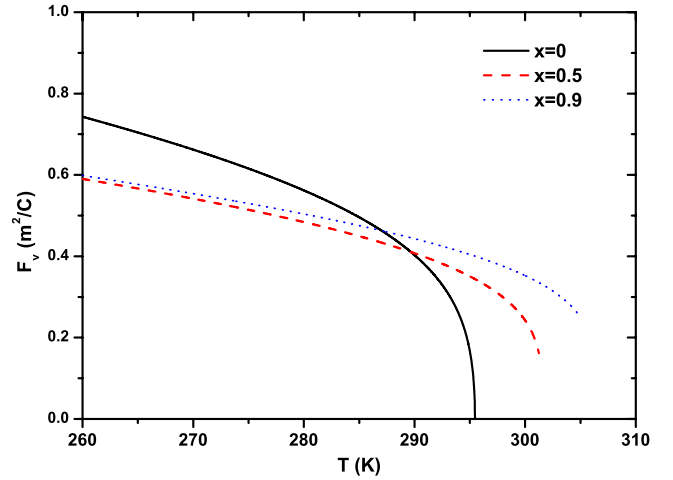


FIG. 8. (Color online) Pyroelectric figure of merit F_v in $(\text{TGSe})_{1-x}(\text{DTGSe})_x$ single crystals with $x=0$, 0.5, and 0.9 obtained from Landau theory.

(coming from the increase in the latent heat) shows that deuteration moves the transition point away from the TCP, thus setting a discontinuous phase transition.

From these values, different thermodynamic quantities can be obtained such as the excess specific heat which is shown in Fig. 1. This figure also shows significant temperatures T_c , T_{tr} , and T_2 . Their relative positions are in agreement with experimental data since phase transition takes place in the range (T_c, T_{tr}) during cooling and within the range (T_{tr}, T_2) during heating.

In the same way, the pyroelectric figure of merit can be obtained. The voltage response of a pyroelectric detector of infrared radiation is given by

$$F_v = \frac{p}{\varepsilon_0 \varepsilon c}, \quad (15)$$

where p is the pyroelectric coefficient, ε is the dielectric permittivity, and c is the volume specific heat. F_v was derived from the Landau potential determined for each sample, by computing the theoretical predictions for p , ε , and c , taking into account the background contribution to the specific heat.

It should be stressed that for ($x=0$) the lack of repeatability in C_{CW} discussed in Sec. III B prevents us from obtaining a suitable value for P_0 . Instead, we have obtained this value from previous data^{2,34} of $P=3.2 \mu\text{C cm}^{-2}$ at $T=273$ K and Eq. (12).

Figure 8 shows the resulting F_v for $(\text{TGSe})_{1-x}(\text{DTGSe})_x$ with $x=0$, 0.5, and 0.9 in the ferroelectric phase. A pyroelectric detector is expected to have higher pyroelectric figure of merit and a plateau in the relevant range of operating temperatures. Parameter F_v for the TGSe sample shows a strong temperature dependence at room temperatures being negligibly small at 295 K which is its upper limit of applicability. This upper limit increases and dF_v/dT decreases with increasing deuteration, making the deuterated samples best suitable for room temperature applications. The $(\text{TGSe})_{1-x}(\text{DTGSe})_x$ system was previously¹⁶ considered as a suitable pyroelectric detector. However, this study did not

account for the influence of deuteration on the specific heat and the analysis was restricted to the behavior of p/ϵ .

Data of F_v at room temperature here presented are, generally speaking, smaller than those obtained¹⁵ for alanine-doped deuterated TGS single crystals, which are used as conventional pyroelectric detectors and, moreover, dF_v/dT is also smaller for alanine-doped deuterated TGS single crystals. At lower temperatures, below 273 K where the value of F_v is higher and seems to reach a more stable value, deuterated TGSe could be considered as a candidate for a pyroelectric detector.

V. CONCLUSIONS

Specific heat, latent heat and dielectric permittivity have been measured for pure, half-deuterated and highly-deuterated TGSe. The analysis of the data has shown that the ferroelectric phase transition of $(\text{TGSe})_{1-x}(\text{DTGSe})_x$ can be described in the framework of a 2-4-6 Landau classical potential. The coefficients of the Landau model for different samples of $(\text{TGSe})_{1-x}(\text{DTGSe})_x$ show that the ferroelectric phase transition is moving away from the TCP as x increases. B decreases and shifts from zero to negative values as a consequence of the increase in the latent heat. On the contrary A and C smoothly change with x .

The pyroelectric figure of merit has been deduced from Landau potential. Deuteration reduces the temperature dependence of F_v and increases the temperature interval where this material could be used as a pyroelectric sensor.

ACKNOWLEDGMENTS

This work has been supported by Project No. FIS2006-04045 of the Spanish Government. The authors wish to thank Dr. J. Jiménez for his support of the experimental device and Dr. M. Koralewski for supplying the samples.

¹B. Březina and F. Smutný, *Czech. J. Phys.* **18**, 393 (1968).

²Z. Málek, I. Štrajblová, J. Novotný, and V. Mereček, *Czech. J. Phys.* **18**, 1224 (1968).

³J. Baran, M. Sledz, R. Jacubas, and G. Bator, *Phys. Rev. B* **55**, 169 (1997).

⁴M. C. Gallardo, J. Jiménez, M. Koralewski, and J. del Cerro, *J. Appl.*

Phys. **81**, 2584 (1997).

⁵C. Aragón and J. A. Gonzalo, *J. Phys.: Condens. Matter* **12**, 3737 (2000).

⁶J. M. Delgado-Sánchez, J. M. Martín-Olalla, M. C. Gallardo, S. Ramos, M. Koralewski, and J. del Cerro, *J. Phys.: Condens. Matter* **17**, 2645 (2005).

⁷T. Kikuta, Y. Kawagishi, T. Yamazaki, and N. Nakatani, *Ferroelectrics* **337**, 95 (2006).

⁸B. T. Matthias, C. E. Miller, and J. Remeika, *Phys. Rev.* **104**, 849 (1956).

⁹F. Jona and G. Shirane, *Ferroelectric Crystals* (Pergamon, New York, 1962).

¹⁰D. J. White, *J. Appl. Phys.* **35**, 3536 (1964).

¹¹A. Hadni, R. Thomas, and J. Perrin, *J. Appl. Phys.* **40**, 2740 (1969).

¹²G. Rosenman, D. Shur, and A. Skliar, *J. Appl. Phys.* **79**, 7401 (1996).

¹³G. Rosenman, D. Shur, Y. E. Krasik, and A. Dunaevsky, *J. Appl. Phys.* **88**, 6109 (2000).

¹⁴S. Hoshino, T. Mitsui, F. Jona, and R. Pepinsky, *Phys. Rev.* **107**, 1255 (1957).

¹⁵S. Ramos, J. M. Martí, and J. del Cerro, *Jpn. J. Appl. Phys., Part 1* **34**, 2389 (1995).

¹⁶M. Wang, C. S. Fang, and H. S. Zhuo, *Ferroelectrics* **91**, 365 (1989).

¹⁷F. J. Romero, M. C. Gallardo, J. Jiménez, M. Koralewski, A. Czarnecka, and J. del Cerro, *J. Phys.: Condens. Matter* **16**, 7637 (2004).

¹⁸K. Gesi, *J. Phys. Soc. Jpn.* **41**, 565 (1976).

¹⁹C. Aragón and J. A. Gonzalo, *Ferroelectr., Lett. Sect.* **27**, 83 (2000).

²⁰Y. W. Song, S. A. Taraskin, and B. A. Strukov, *J. Korean Phys. Soc.* **27**, S73 (1994).

²¹Y. W. Song, J. C. Kim, I. K. You, and B. A. Strukov, *Mater. Res. Bull.* **35**, 1087 (2000).

²²F. J. Romero, M. C. Gallardo, and J. del Cerro, *Europhys. Lett.* **76**, 863 (2006).

²³F. J. Romero, M. C. Gallardo, and J. del Cerro, *J. Phys.: Condens. Matter* **21**, 155902 (2009).

²⁴J. del Cerro, J. M. Martín-Olalla, and F. J. Romero, *Thermochim. Acta* **401**, 149 (2003).

²⁵F. J. Romero, M. C. Gallardo, A. Czarnecka, M. Koralewski, and J. del Cerro, *J. Therm. Anal. Calorim.* **87**, 355 (2007).

²⁶J. del Cerro, F. J. Romero, M. C. Gallardo, S. A. Hayward, and J. Jiménez, *Thermochim. Acta* **343**, 89 (2000).

²⁷F. J. Romero, M. C. Gallardo, S. A. Hayward, J. Jiménez, J. del Cerro, and E. K. H. Salje, *J. Phys.: Condens. Matter* **16**, 2879 (2004).

²⁸M. C. Gallardo, J. Jiménez, and J. del Cerro, *Rev. Sci. Instrum.* **66**, 5288 (1995).

²⁹J. del Cerro, *J. Therm. Anal.* **34**, 335 (1988).

³⁰A. Czarnecka and J. Stankowska, *Ferroelectr., Lett. Sect.* **1**, 163 (1984).

³¹B. Fugiel and M. Mierzwa, *Phys. Rev. B* **57**, 777 (1998).

³²S. A. Hayward, F. J. Romero, M. C. Gallardo, J. del Cerro, A. Gibaud, and E. K. H. Salje, *J. Phys.: Condens. Matter* **12**, 1133 (2000).

³³M. C. Gallardo, F. J. Romero, S. A. Hayward, E. K. H. Salje, and J. del Cerro, *Miner. Mag.* **64**, 971 (2000).

³⁴F. Jona and G. Shirane, *Phys. Rev.* **117**, 139 (1960).